Int. J. Solids Structures, 1966, Vol. 2, pp. 223 to 233. Pergamon Press Ltd. Printed in Great Britain

ON FINITE DEFLECTION OF AN EXTENSIBLE CIRCULAR RING SEGMENT

R. P. NORDGREN
Shell Development Company, Houston, Texas

Abstract—The classical elastica is applied to the finite deflection of a segment of an extensible circular ring with clamped ends under a centrally directed concentrated force at the midpoint about which symmetry prevails. Numerical results are presented for rings subtending angles of 90° and 14·7°. A solution obtained by the theory of shallow rings shows excellent agreement with the exact results for the 14·7° case. Agreement with experiment is satisfactory for both angles.

INTRODUCTION

THE FINITE deflection of a circular ring segment (arch) with clamped ends under a centrally directed concentrated force at the midpoint (Fig. 1) is of both theoretical and technical interest.* Van Wijngaarden [1] gives an analysis and numerical results for a semicircular inextensible ring with deflection symmetric about the midpoint, and this case is also treated by Frisch-Fay [2], who uses the classical elastica. For a shallow extensible ring, Gjelsvik and Bodner [3] have studied nonsymmetric as well as symmetric deflection by energy methods. Also, experimental findings are reported in [1] and [3].

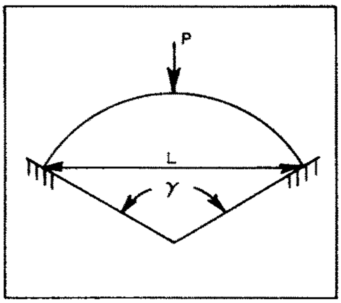

FIG. 1. Undeflected beam.

The present paper applies the classical elastica† to the problem for symmetric deflection of an extensible ring segment subtending an angle γ. The problem is reduced to the solution of a transcendental equation in elliptic integrals, and numerical results are presented for $\gamma = 90°$ and $\gamma = 14{\cdot}7°$. By the theory of shallow beams, a solution in elementary functions is also obtained which for $\gamma = 14{\cdot}7°$ predicts the central force to

* For example, such rings are used in their deflected states as springs with negative spring constants in combination with ordinary springs in seismic instruments.

† Numerous applications of the elastica appear in the literature. References are cited in [2, 4] and the review article [7] and more recent applications can be found in [8–10].

within 0·5 per cent of the exact solution at the same midpoint deflection. The theoretical central force is within 10 per cent of experimental values reported here for $\gamma = 90°$ and in [3] for $\gamma = 14{\cdot}7°$.

ANALYSIS

The analysis is based on the classical Bernoulli–Euler theory of flexure with Hooke's law relating tension and extension. The constitutive equations for plane deflection can be written as ([4] pp. 394, 401)

$$M = B(\kappa - \kappa_0), \qquad B \equiv EI, \tag{1a}$$

$$T = EA\varepsilon, \tag{1b}$$

where M, T, κ_0, E, A, and I denote stress couple, tension, initial curvature of the centroidal axis*, Young's modulus, cross-sectional area, and second moment of area, respectively; the latter four are taken constant. The curvature κ and strain ε of the deformed central axis are defined here by

$$\kappa = \frac{\mathrm{d}\theta}{\mathrm{d}s}, \tag{1c}$$

$$\varepsilon = \frac{\mathrm{d}s - \mathrm{d}s'}{\mathrm{d}s}, \tag{1d}$$

where s and s' are the arc lengths along the central axis from a specific point in the deformed and undeformed states, respectively, and θ is the slope angle of the central axis. It should be noted that (1d) may also be written as

$$\varepsilon = \left(\frac{\mathrm{d}s - \mathrm{d}s'}{\mathrm{d}s'}\right)(1-\varepsilon),$$

where the first factor on the right-hand side is an alternative definition of strain; however, the difference is immaterial for $\varepsilon \ll 1$. When (1a) and (1c) are combined with the equations of equilibrium for beams under a force resultant R applied at the ends, the following differential equation for θ results ([4] p. 401):

$$B\frac{\mathrm{d}^2\theta}{\mathrm{d}s^2} + R\sin\theta = 0, \tag{2a}$$

where θ is measured from the axis x of a rectangular Cartesian coordinate system x, y with x in the direction of R (Fig. 2). The coordinates satisfy the geometrical equations

$$\frac{\mathrm{d}x}{\mathrm{d}s} = \cos\theta, \qquad \frac{\mathrm{d}y}{\mathrm{d}s} = \sin\theta. \tag{2b}$$

The solution of (2) for x, y, and θ may be accomplished in terms of elliptic functions [4] or elliptic integrals [2] and takes a different form according to whether or not inflection points are present. The solution curves, known as elastica, were studied by James Bernoulli and by Euler (see [5]).

* The present analysis and the previous ones [1–3] also may be applied to an initially straight beam which is first bent to circular form by pure end couples. In this case κ_0 is absent from (1a).

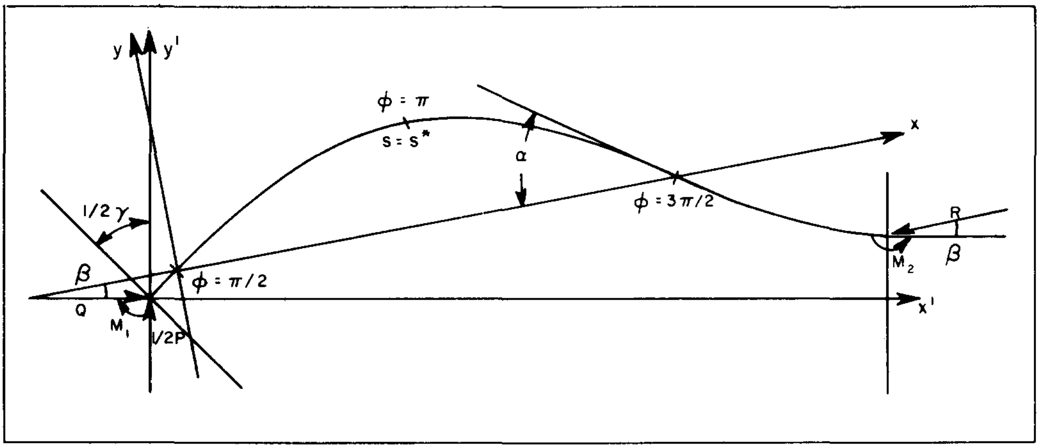

FIG. 2. Left half of deformed beam with notation.

In the present problem, by virtue of symmetry, only one-half of the ring segment need be considered, and since this half is acted on only by end forces and couples, the plane deflection curves are portions of elastica. Although the initial circular arc is a noninflectional elastica, the inflectional case is found to apply for all except extremely small deflections*; therefore, the solution will be formulated for this case.

Taking the origin of the x, y system at an inflection point (Fig. 2), we can write the equations of the inflectional elastica as [2, 4]

$$\begin{aligned} x &= \sqrt{\frac{B}{R}}\left[F\left(\frac{\pi}{2},k\right)-F(\phi,k)-2E\left(\frac{\pi}{2},k\right)+2E(\phi,k)\right], \\ y &= -2k\sqrt{\frac{B}{R}}\cos\phi, \qquad \sin\frac{\theta}{2} = k\sin\phi, \\ s &= \sqrt{\frac{B}{R}}\left[F(\phi,k)-F\left(\frac{\pi}{2},k\right)\right], \qquad k = \sin\frac{\alpha}{2}, \end{aligned} \tag{3}$$

where α is the slope angle at the origin, and $F(\phi,k)$ and $E(\phi,k)$ are incomplete elliptic integrals of the first and second kind, respectively, of modulus k and unrestricted argument ϕ. The x, y coordinate system moves as the beam deflects and is related to the fixed coordinate system x', y', shown in Fig. 2, by the transformation

$$\begin{aligned} x' &= [x-x(s_1)]\cos\beta-[y-y(s_1)]\sin\beta, \\ y' &= [x-x(s_1)]\sin\beta+[y-y(s_1)]\cos\beta, \end{aligned} \tag{4}$$

where β is the angle between the x and x' axes, and s_1 is the value of s at the left clamped end. By equilibrium and symmetry, and since the ends of the beam are immovably clamped a distance L apart, we have

$$P = 2R\sin\beta, \tag{5}$$

$$\theta(s_1) = \tfrac{1}{2}\gamma-\beta, \qquad \theta(s_2) = -\beta, \tag{6}$$

$$x'(s_2)-x'(s_1) = \tfrac{1}{2}L, \tag{7}$$

* For such small deflections the linear theory of circular rings should be adequate.

where P, γ, and s_2 are, respectively, the magnitude of the concentrated central force, the opening angle, and the value of s at the midpoint of the beam. The deflection at the midpoint, measured from the initial circular arc, is given by

$$\delta = \tfrac{1}{2}L\tan\tfrac{1}{4}\gamma - y'(s_2). \tag{8}$$

By equilibrium (Fig. 2)

$$T = -R\cos\theta,$$

and by (1b, c) we have

$$\left(1+\lambda^2\frac{L^2R}{B}\cos\theta\right)ds = ds', \qquad \lambda = \frac{1}{L}\sqrt{\frac{I}{A}},$$

which, when integrated from $s = s_1$ to $s = s_2$ with the aid of (2b), yields

$$s_2 - s_1 + [x(s_2) - x(s_1)]\lambda^2\frac{L^2R}{B} = \frac{\frac{1}{4}\gamma L}{\sin\frac{1}{2}\gamma}. \tag{9}$$

According to (9), results for an inextensible beam can be obtained by setting $\lambda = 0$ in the equations which follow.

By (3) and (6) it follows that

$$\begin{aligned} \phi(s_1) &= m\pi + (-1)^m \arcsin[k^{-1}\sin\tfrac{1}{2}(\tfrac{1}{2}\gamma-\beta)], \\ \phi(s_2) &= n\pi - (-1)^n \arcsin[k^{-1}\sin\tfrac{1}{2}\beta], \end{aligned} \tag{10}$$

where m and n take integer values and

$$-\frac{\pi}{2} < \arcsin[\quad] \leq \frac{\pi}{2}.$$

It is easily shown that the arguments of the arcsin functions in (10) lie in the interval -1, $+1$, provided that

$$\tfrac{1}{2}\gamma - \alpha \leq \beta \leq \alpha. \tag{11}$$

Equations (3), (4), and (9) lead to

$$F(\phi_2, k) - F(\phi_1, k) + \lambda^2 A^2 G(\phi_1, \phi_2, k) - \frac{\frac{1}{2}\gamma A}{\sin\frac{1}{2}\gamma} = 0, \tag{12}$$

where

$$G(\phi_1, \phi_2, k) = F(\phi_1, k) - F(\phi_2, k) - 2E(\phi_1, k) + 2E(\phi_2, k),$$

$$\phi_1 \equiv \phi(s_1), \qquad \phi_2 \equiv \phi(s_2), \qquad A \equiv L\sqrt{\frac{R}{B}},$$

and by (7)

$$A = 2G(\phi_1, \phi_2, k)\cos\beta + 4k[\cos\phi_2 - \cos\phi_1]\sin\beta.$$

For given values of γ and λ, (10) and (12) can be solved numerically in the range (11) for β as a function of k with specific m and n. With β known, the central force and midpoint deflection are given by (5) and (8) in the nondimensional form

$$\frac{PL^2}{B} = 2A^2 \sin\beta,$$

$$\frac{\delta}{L} = \tfrac{1}{2}\tan\tfrac{1}{4}\gamma - A^{-1}G(\phi_1, \phi_2, k)\sin\beta + 2kA^{-1}[\cos\phi_2 - \cos\phi_1]\cos\beta, \tag{13}$$

and by (2), (3), and (13) the curvature κ of the beam is

$$\frac{\kappa}{\kappa_0} = \frac{A\sin\frac{1}{2}\alpha\cos\phi}{\sin\frac{1}{2}\gamma}, \qquad \kappa_0 \equiv \frac{L}{2\sin\frac{1}{2}\gamma}, \tag{14}$$

where κ_0 is the curvature of the undeflected circular ring. Numerical results will be discussed in the last section.

SHALLOW BEAMS

If the beam is shallow, i.e. if $\gamma \ll 1$, then the slope $\mathrm{d}y'/\mathrm{d}x'$ is expected to be small, and the approximation

$$\kappa = \frac{\mathrm{d}^2y'}{\mathrm{d}x'^2}\left[1+\left(\frac{\mathrm{d}y'}{\mathrm{d}x'}\right)^2\right]^{-\frac{3}{2}} \simeq \frac{\mathrm{d}^2y'}{\mathrm{d}x'^2}$$

may be invoked, in which case (1) and moment equilibrium (Fig. 2) yield

$$B\frac{\mathrm{d}^2y'}{\mathrm{d}x'^2} + Qy' = M(s_1) + \tfrac{1}{2}Px', \tag{15}$$

where Q is the compressive force parallel to the x' axis (Fig. 2). For $Q > 0$, the general solution of (15) is

$$\frac{y'}{L} = C_1\sin\eta\frac{x'}{L} + C_2\cos\eta\frac{x'}{L} + \mu + \frac{\rho x'}{2L}, \tag{16}$$

where

$$\eta = L\sqrt{\frac{Q}{B}}, \qquad \rho = \frac{P}{Q}, \qquad \mu = \frac{M(s_1)}{QL}.$$

The constants μ, C_1, and C_2 are determined by the conditions

$$y'(0) = \frac{\mathrm{d}y'}{\mathrm{d}x'}\left(\frac{L}{2}\right) = 0, \qquad \frac{\mathrm{d}y'}{\mathrm{d}x'}(0) = \tfrac{1}{2}\gamma \tag{17}$$

as

$$C_1 = \frac{1}{2\eta}(\gamma - \rho), \tag{18a}$$

$$C_2 = -\mu = \frac{1}{2\eta}[\gamma\cot\tfrac{1}{2}\eta + \rho\tan\tfrac{1}{4}\eta]. \tag{18b}$$

By (4), we have

$$x(s_2)-x(s_1) = \frac{L}{2}\cos\beta+y'\left(\frac{L}{2}\right)\sin\beta,$$

and since (Fig. 2)

$$R = \frac{Q}{\cos\beta} = \frac{P}{2\sin\beta},$$

(9) is equivalent to

$$\int_0^{L/2}\sqrt{\left[1+\left(\frac{\mathrm{d}y'}{\mathrm{d}x'}\right)^2\right]}\,\mathrm{d}x'+\frac{LQ}{2EA}+\frac{P}{2EA}y'\left(\frac{L}{2}\right) = \frac{\frac{1}{4}\gamma L}{\sin\frac{1}{2}\gamma},$$

which for shallow beams can be approximated by

$$\frac{1}{L}\int_0^{L/2}\left(\frac{\mathrm{d}y'}{\mathrm{d}x'}\right)^2\mathrm{d}x'+\frac{Q}{EA}+\frac{P}{EAL}y'\left(\frac{L}{2}\right) = \frac{\gamma^2}{24}. \tag{19}$$

Substitution of (16) and (18) into (19) leads to the quadratic equation

$$a\rho^2+b\rho+c = 0, \tag{20}$$

where

$$a = \frac{1}{16\eta}[3\eta-\sin\eta-4\sin\tfrac{1}{2}\eta+\tan^2\tfrac{1}{4}\eta(\eta-\sin\eta-8\sin\tfrac{1}{2}\eta)]$$
$$+\lambda^2\eta\left[\frac{\eta}{4}-\tfrac{1}{2}\tan\tfrac{1}{4}\eta\right],$$

$$b = \frac{\gamma}{8\eta}[2(1+2\cos\tfrac{1}{2}\eta)\sin\tfrac{1}{2}\eta-\eta-\sin\eta]$$
$$+\tfrac{1}{2}\lambda^2\eta\gamma\tan\tfrac{1}{4}\eta,$$

$$c = \frac{\gamma^2(\eta-\sin\eta)}{16\eta\sin^2\frac{1}{2}\eta}+\eta^2\lambda^2-\tfrac{1}{24}\gamma^2,$$

and λ is defined at (12). Thus, for each value of η, (20) will give two real values of ρ, provided that $b^2-4ac > 0$. Then, by (16) and (18) the central force and midpoint deflection are given by

$$\frac{PL^2}{B} = \rho\eta^2,$$

$$\frac{\delta}{L} = \tfrac{1}{8}\gamma-\tfrac{1}{4}\rho+\frac{1}{2\eta}(\gamma+2\rho)\tan\tfrac{1}{4}\eta \tag{21}$$

The foregoing solution can also be applied for $Q < 0$ merely by transforming the trigonometric functions to hyperbolic functions. Furthermore, as $Q \to 0$ it can be shown that the foregoing solution approaches the polynomial solution in x' obtainable directly from (15) for $Q = 0$.

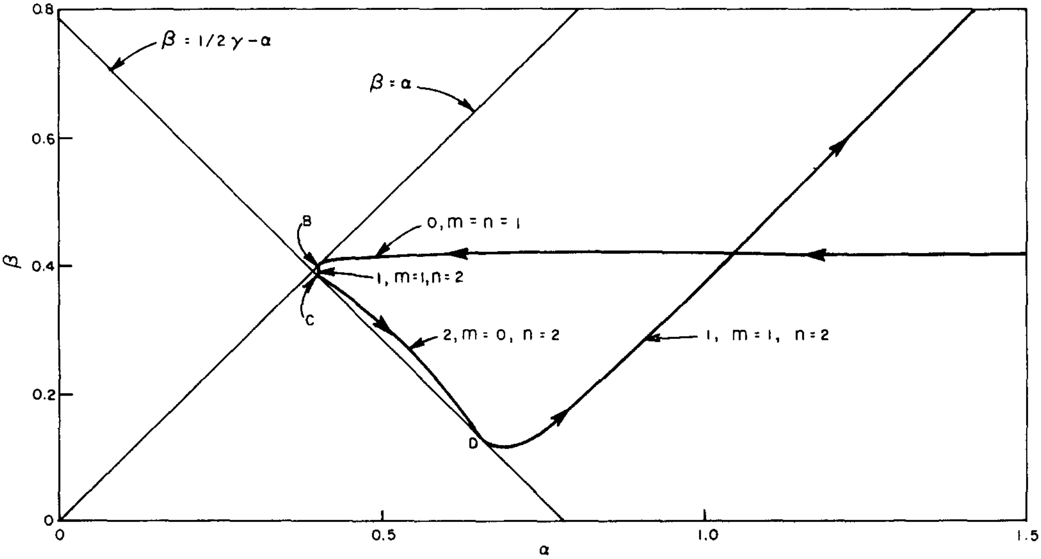

FIG. 3. β versus α (in radians) for $\gamma = 90°$ and $\lambda = 0$; the first number for each section is the number of inflection points on the half-beam.

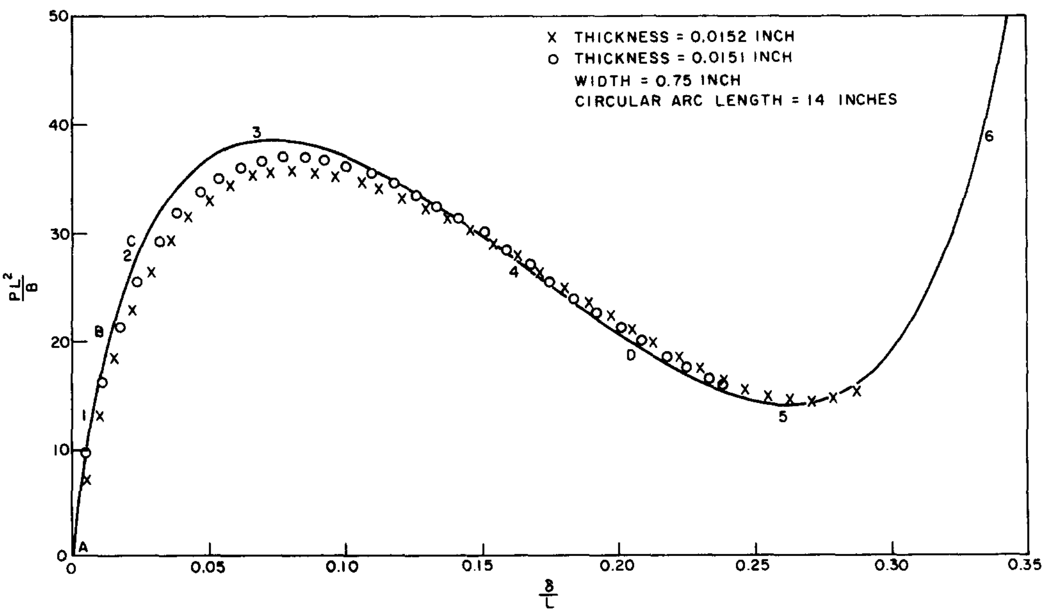

FIG. 4. Central force versus midpoint deflection for $\gamma = 90°$ and $\lambda = 0$ (solid line).

DISCUSSION OF NUMERICAL AND EXPERIMENTAL RESULTS

Numerical results were obtained on a digital computer with the subroutines for elliptic integrals given by Hofsommer and van de Riet [6].

For the case $\gamma = 90°$ and $\lambda = 0$ (extension neglected) Figs. 3 and 4 show, respectively, β versus α and the relation between central force and midpoint deflection in nondimensional form as obtained from (10) through (13). In Fig. 3 the arrows indicate increasing midpoint deflection, and for each section of curve the number of inflection points on the half-ring and the corresponding values of m and n in (10) are given. At the transition points C and D in Figs. 3 and 4 inflection points occur at the ends of the half-ring. The transition from noninflectional elastica to inflectional elastica occurs at point A in Fig. 4 for $\alpha = \pi$ and $\delta/L = 1{\cdot}90 \times 10^{-3}$, which is small, as stated previously.* Typical deflection curves for the left half-beam appear in Fig. 5 corresponding by number to points on the force-deflection curve of Fig. 4. Inflection points in Fig. 5 are indicated by circles.

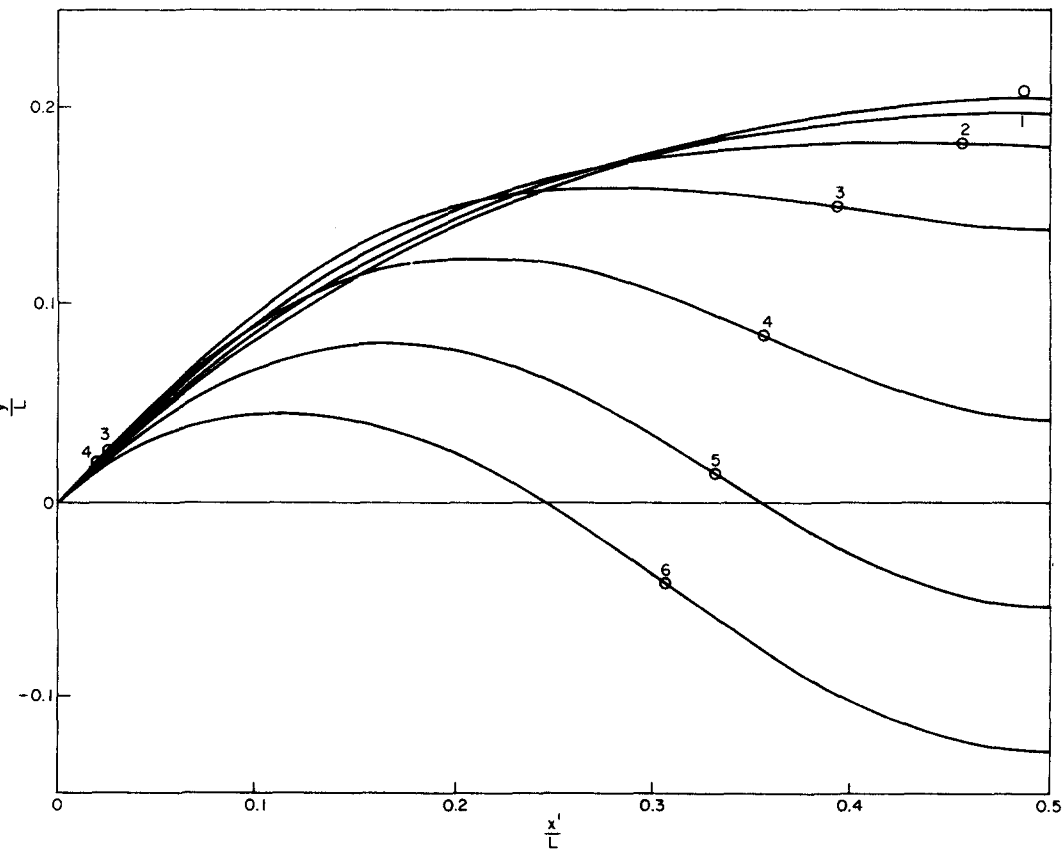

FIG. 5. Deflection curves of the left half-beam for $\gamma = 90°$ and $\lambda = 0$ corresponding by number to load points in Fig. 4; circles denote inflection points.

* The discussion by Frisch-Fay ([2] p. 145) of the various changes in character of the deflection curve for a semicircular beam ($\gamma = 180°$) applies for $\gamma = 90°$ and $14{\cdot}7°$ and appears to apply for $0 < \gamma \leq 180°$.

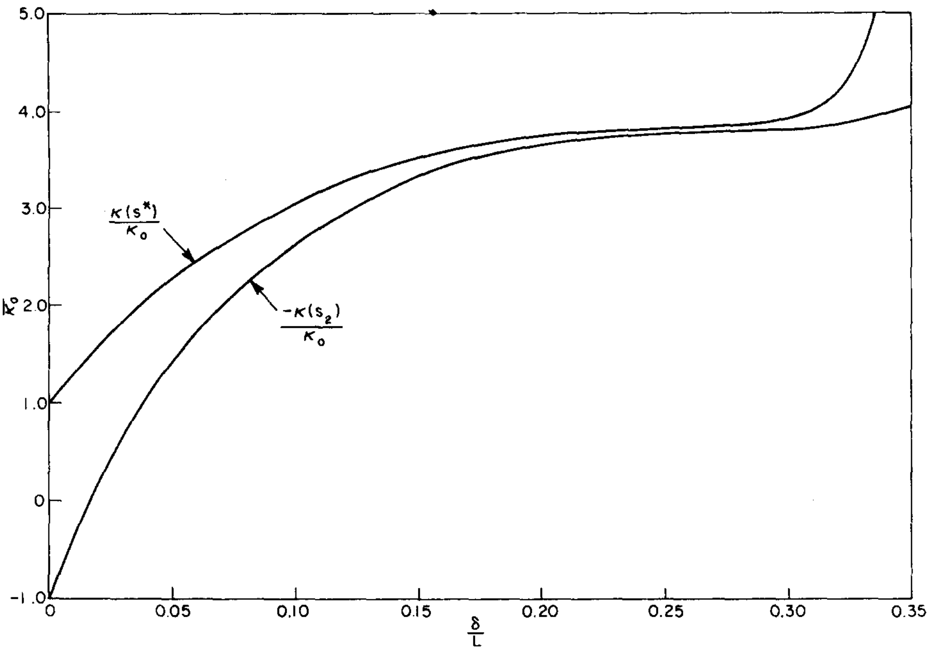

FIG. 6. Maximum curvature $\kappa(s^*)$ and minimum curvature $\kappa(s_2)$ versus midpoint deflection; κ_0 is curvature in circular state for $P = \delta = 0$.

The relation between central force and midpoint deflection was also computed for $\gamma = 90°$ including the effect of extension with $\lambda = 0{\cdot}00095$ (as in the experiment reported here). The difference in central force between this case and the inextensional case ($\lambda = 0$) for the same midpoint deflection is less than 0·3 per cent over the range of Fig. 3.

Figure 6 shows curvature ratios for $\gamma = 90°$ and $\lambda = 0$ as obtained from (14) at the point of minimum curvature $s = s_2$ and at the point of maximum curvature $s = s^*$ ($\phi = \pi$), plotted versus midpoint deflection. These curves can be used to calculate stress due to bending which predominates over direct stress in general.

Similar computations were carried out for $\gamma = 14{\cdot}7°$ including extension with $\lambda = 0{\cdot}00159$ (as in the experiment of [3]) and neglecting extension ($\lambda = 0$). The central force–midpoint deflection relations appear in Fig. 7 and show a maximum difference of 5 per cent in PL^2/B between the two cases. Thus, the effect of extension is more pronounced for $\gamma = 14{\cdot}7°$ than for $\gamma = 90°$. The force–deflection relation for $\gamma = 14{\cdot}7°$ and $\lambda = 0{\cdot}00159$ according to the shallow-beam solution (20) and (21) agrees with the exact solution to within 0·5 per cent in PL^2/B over the range of Fig. 7. In the shallow-beam solution trigonometric functions apply for $0 < \delta/L < 0{\cdot}0533$, and hyperbolic functions apply for $\delta/L > 0{\cdot}0533$, with $b^2 - 4ac = 0$ at $\delta/L = 0{\cdot}0249$, $\eta = 9{\cdot}01$.

Experimental results† shown in Fig. 4 were obtained with beams of thickness 0·0151 in. and 0·0152 in., width 0·75 in., and circular arc length 14 in. ($\lambda \simeq 0{\cdot}00095$) by varying the midpoint deflection and measuring the central force with a spring gauge. Nonsymmetric deflections were suppressed by clamping and restraining a central portion of the beam.

† The experiments were conducted under the direction of M. M. Robinson and R. R. Luke of Shell Development Co.

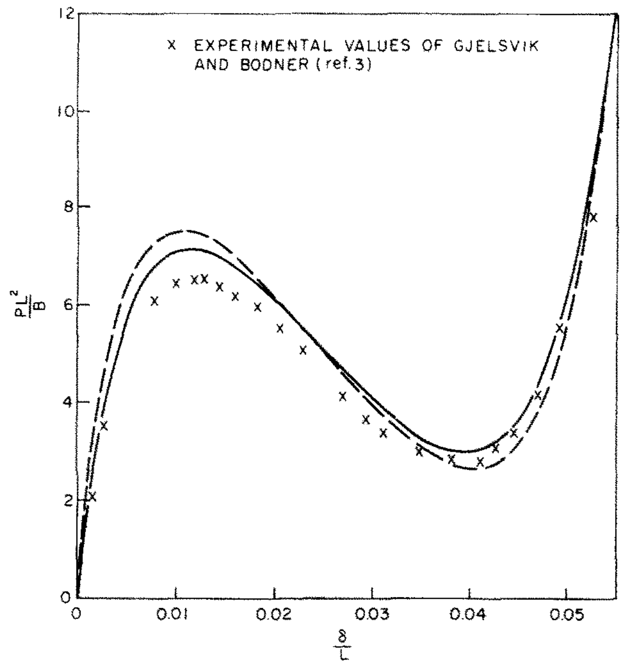

FIG. 7. Central force versus midpoint deflection for $\gamma = 14{\cdot}7°$, $\lambda = 0$ (dashed line), and $\lambda = 0{\cdot}00159$ (solid line).

The discrepancy between theoretical and experimental central force for the same midpoint deflection is less than 10 per cent and is believed to be due largely to incomplete suppression of nonsymmetric deflection. The experimental results reported in [3] for a beam with $\gamma = 14{\cdot}7°$ and $\lambda = 0{\cdot}00159$ are also shown in Fig. 7. In this experiment slight nonsymmetric deflection occurred which may account for the difference with theory.

REFERENCES

[1] A. VAN WIJNGAARDEN, Large distortions of circular rings and straight rods. *Proc. Kned. Akad. Wet.* **49**, 648 (1946).

[2] R. FRISCH-FAY, *Flexible Rods*. Butterworths (1962).

[3] A. GJELSVIK and S. R. BODNER, The energy criterion and snap buckling of arches. *J. Engng Mech. Div. Am. Soc. Civ. Engrs* **88**, 87 (1962).

[4] A. E. H. LOVE, *A Treatise on the Mathematical Theory of Elasticity*, 4th edition. Dover (1944).

[5] C. TRUESDELL, *The Rational Mechanics of Flexible or Elastic Bodies*, 1638–1788, Ser. II, vol. 11, pt. 2, 435 pp. Orell Füssli, Zürich (1960).

[6] D. J. HOFSOMMER and R. P. VAN DE RIET, On the numerical calculation of elliptic integrals of the first and second kind and the elliptic functions of Jacobi. *Num. Math.* **5**, 291 (1963).

[7] J. G. EISLEY (1963), Nonlinear deformation of elastic beams, rings and strings. *Appl. Mech. Rev.* **16**, 667 (1963).

[8] G. E. SLITER and A. P. BORESI, Elastica supported at midpoint by a spring. *J. Engng Mech. Div., Am. Soc. civil Engrs* **90**, 1 (1964).

[9] C. N. KERR, Large deflections of a square frame. *Q. Jl. Mech. Appl. Math.* **17**, 23 (1964).

[10] CHIEN-HENG WU and R. PLUNKETT, On the contact problem of thin rings. *J. Appl. Mech.* **32**, 11 (1965).

(*Received* 24 *May* 1965)

Résumé—L'élastica classique est appliquée à la flexion (déformation) finie d'un segment d'un anneau circulaire extensible à extrémités bridées sous une force concentrée centralement dirigée au point milieu où la symétrie prédomine. Des résultats numériques y sont présentés pour des anneaux soutendant des angles de 90° et 14,7°. Une solution obtenue avec la théorie pour anneaux peu profonds indique une conformité excellente avec les résultats exacts pour le cas de 14,7°. La conformité avec l'expérience est satisfaisante pour les deux angles.

Zusammenfassung—Die klassische Theorie der Elastika ist angewendet auf die endliche Biegung eines Segments eines dehnbaren kreisförmigen Ringes mit geklemmten Enden bei einer zentral gerichteten konzentrierten Kraft an dem Mittelpunkt an welchem Symmetrie vorliegt. Zahlemmässige Ergebnisse sind präsentiert für gegenüberliegende Ringwinkel von 90° und 14,7°. Eine Lösung, erhalten mit der Theorie von flachen Ringen zeigt ausgezeichnete Übereinstimmung mit den genauen Ergebnissen für den 14,7° Fall. Übereinstimmung mit dem Versuch ist zufriedenstellend für beide Winkel.

Абстракт—Классическая теория эластики применяется при конечном изгибании сегмента растяжимого круглого кольца с зажатыми концами под направленной к центру концентрированной силой в среднем пункте с преобладающей симметрией. Представлены числовые результаты для углов, подпирающих кольца в 90° и 14·7°. Решение, полученное при теории поверхностных колец показывает прекрасное согласование с точными результатами для случая в 14·7°. Согласованность с экспериментом удовлетворительна для обоих углов.